NASA TT F-12,121

INTERFEROMETRIC STUDY OF A MACH 5 FLOW AROUND A SPHERE

JEAN LOUIS SOLIGNAC

Translation of: "Etude interferometrique de l'ecoulement a Mach 5 autour d'une sphere"
Office National D'Etudes Et De Recherches Aerospatiales, T.P. 624,
La Recherche Aerospatiale No.125, Jul-Aug 1968,
pp 31-39 + errata

NATIONAL AERONAUTICS AND SPACE ADMINISTRATION
WASHINGTON, D.C. MARCH 1969

INTERFEROMETRIC STUDY OF A MACH 5 FLOW AROUND A SPHERE[1]

Jean Louis Solignac

ABSTRACT: A Mach 5 flow around a sphere was investigated by interferometry. The conditions for use of an interferogram of an axisymmetric flow, in the presence of a shock, are given. A program for calculating the flow downstream of a shock was established on the basis of an experimental determination of specific measurements in the field unstudied. The results of these calculations are in excellent agreement with those corresponding to the second approximation of the Belotserkowsky method.

1. Introduction

The application of interferometry to an analysis of the flow /31* around projectiles has already been the subject of several detailed studies.

If the first publications, particularly those by Ladenburg, Van Voorhis and Winckler [1], have given general elements of the use of this experimental techniques since 1946, the studies which appeared after that brought improvements both in the quality of measurements carried out under varying conditions and in practical use of this method:

- Wood and Gooderum [2] published a study on the sphere in 1950 which gave a clear and detailed review of the method and analysis, together with explanations for the errors.

- Bennett, Carter and Bergdolt [3] studied the flow around /32 cones and spheres in free flight, which had been analyzed before in wind tunnels, in order to obtain pure experimental conditions. They also showed a method of considering the singularity of the interferometry method due to the discontinuity in the specific mass at right angles with the shock. This point had also been examined before, in 1945, by Weyl [4].

- More recently, in 1960, Sedney and Kahl [5] published these results of a study on a sphere for hypersonic flow in a wind tun-

---

* Numbers in the margin indicate pagination in the foreign text.

1 Study carried out with the aid of the Military Engineer J.C. Chaugny of the National Superior School of Armament.

nel with gases of different natures.

- Since 1964, interferometry has been used continuously at the O.N.E.R.A. for internal studies of an axisymmetric flow according to the method defined previously in [6].

This is an example of the general method in the frequently-encountered case where the flow to be studied has one or several shock waves (supersonic flows around blunt obstacles, separation, attachment, etc.).

The case for this study is a flow at M = 5 around a sphere.

This choice was justified by the advantages found both in the realization of a model of small dimensions with great precision and in the definition of a reference flow as a standard. For this purpose, the calculation method of Belotserkowsky [7] was used.

This method, whose experimental confirmation has already been well established [8], has a sufficiently rigid basis for the theory to be considered here as a reference in judging the precision of the measuring techniques used.

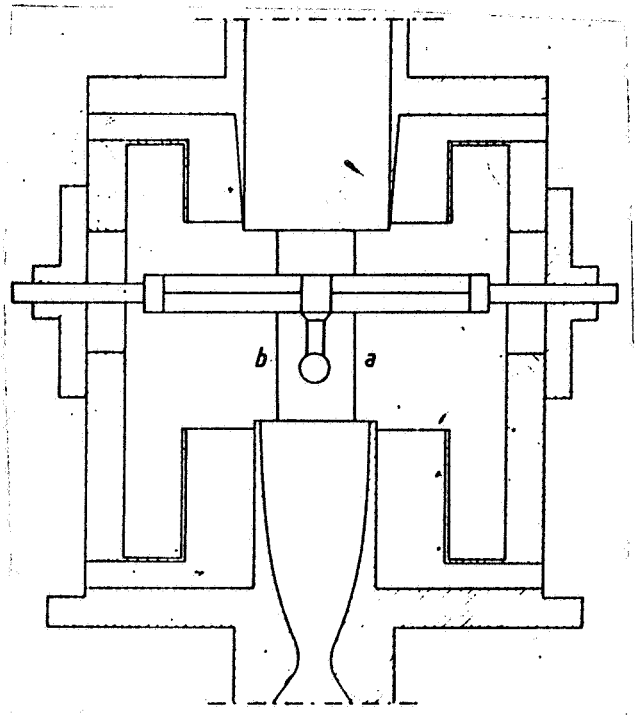

Fig. 1. Flow Diagram. Generating Conditions: Pressure p_{i0} = 15.71 bars, Temperature T_{i0} = 309.8°K.

II. Experimental Study with Wind Tunnel

The tests were carried out with the wind-tunnel S 18 of Chalais-Meudon.

The jet was designed particularly for interferometric studies of axisymmetric flows.

Adjustment of the nozzles and models was guaranteed by the structure. The two wires in the jet, a and b, which are visible in the optical fields, aid in fixing the axis and the scale of the negatives.

Figure 1 shows a schematic diagram of the model (diameter 2a = 8 mm) in the quasi-uniform part of the flow produced by a revolving nozzle (diameter of 30 mm).

An interferogram of the flow which is established around the sphere is represented in Figure 2.

This interferogram was obtained by using the so-called "sharp fringe" control, which produces a picture of fringes parallel to the axis of rotation at the end.

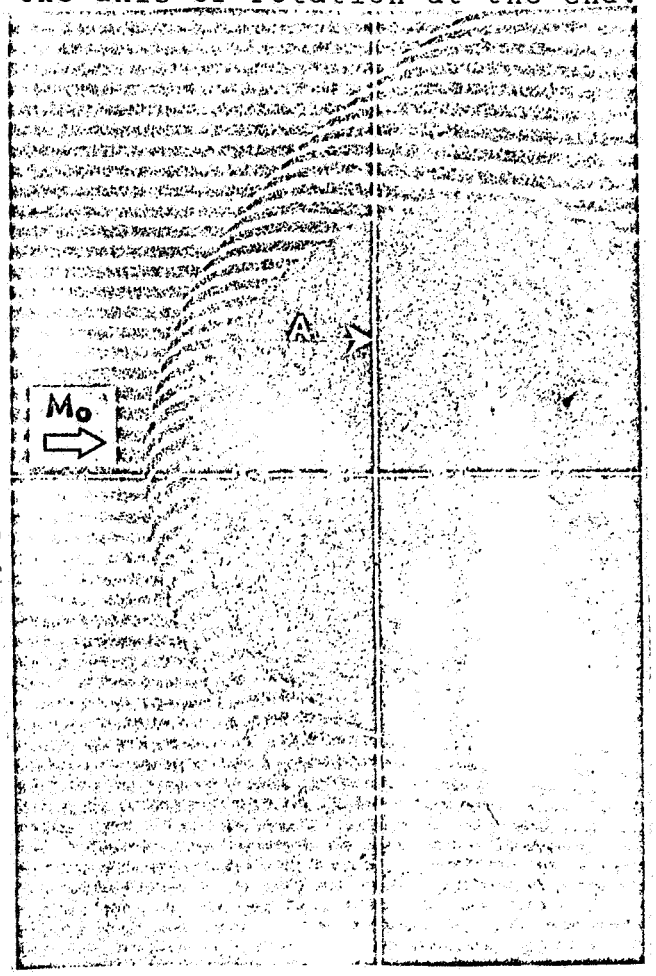

Fig. 2. Interferogram. Emulsion: AGFA 21 DIN. Exposure time, 1/400 sec; Radiation used, Green Line (λ = 5461 Å) Of a Mercury-Vapor Lamp Isolated by a Wratten 77 Filter. A = Scanning Line.

The use of stagnation pressures, with no model in two right-hand sections encompassing the test range, allowed us to determine with precision the disturbances coming from small imperfections in the nozzle, which could make slight modifications in the field around the model.

III. Use of Interferometry

III, 1. General Devices

The mode of interferometric control used allowed us to obtain sufficient information in order to define small variations in the specific mass according to points at the middle of fringes. Nevertheless, the precision of the marker imposed a limit on the initial tightness.

The experimental curves for $N(y)$ and $\bar{N}(y)$, which were obtained with and without wind with a reference of the middle of a fringe of order N, permitted us to define the variation in $S(y) = \bar{N}(y) - N(y)$ along a scanning line normal to the axis due to the aerodynamic field, between the considered point on this line, of the ordinate y, and a reference point. /34

Since the specific mass on the side upstream of the shock wave was known from data determined in the probing of the nozzle, interferometry aided in measuring its variation over the entire section normal to the axis, between the shock and the profile.

An advantageous simplification is found during a study carried out in the vicinity of the axis in a uniform axisymmetric flow upstream of the obstacle. In this case, the optical path

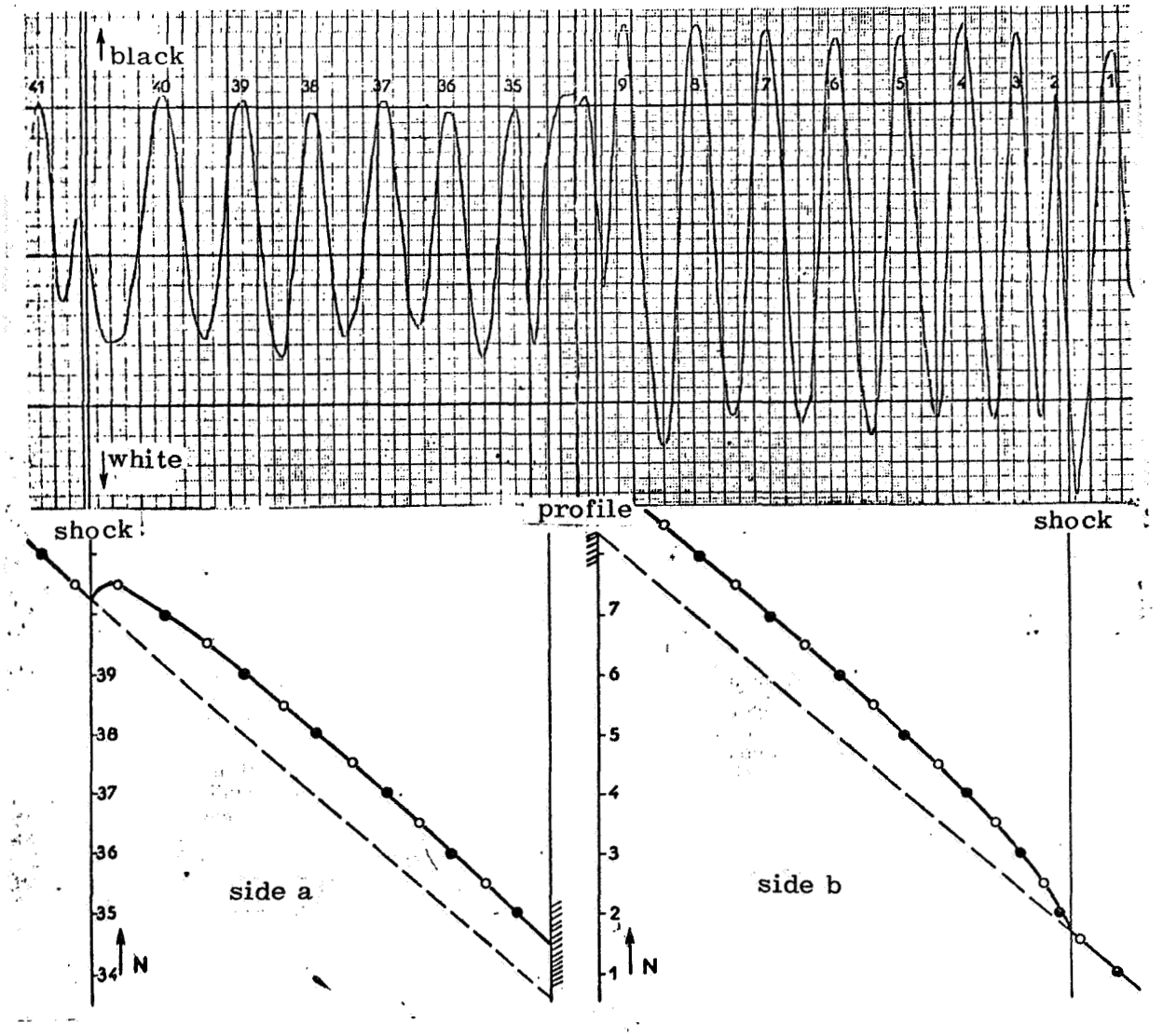

Fig. 3. Densitometric Reading of Negative.
A = Scanning Line.

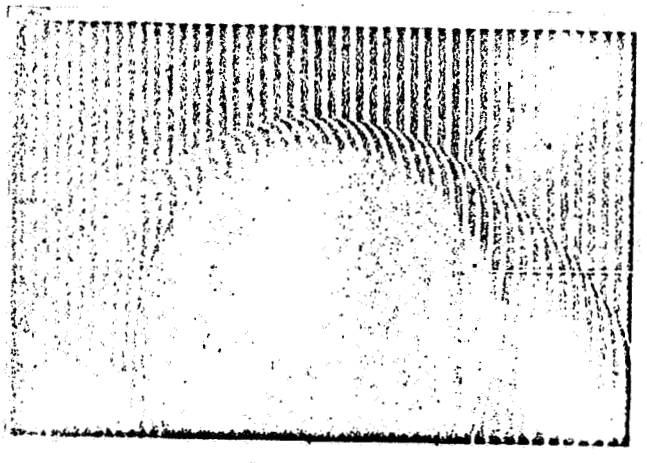

Fig. 3b.

varies little from one point to another in the neighborhood of the axis upstream of the shock, and the picture of the fringes on the negative of the flow reproduces the reference table without flow in this region after it is turned.

Considering this property, $\bar{N}(y)$ was obtained for each scanning line by extrapolation of the line $N(y)$ given by the picture of the outer fringes in the region inside the shock

wave (dotted line in Figure 3).

Thus, a single negative of an interferogram is used for analysis, which is advantageous both for the studies and for precision in the results.

The curve of N(y) is determined on the basis of a localization of middle points of the fringes (maxima and minima of optical density) with precision of ± 0.01, with the aid of a Joyce Loebl microdensitometer.

III. 2. Use of Measurements of Axisymmetric Flow.

An interferogram of an axisymmetric flow is used in determining the specific mass in a meridian section, on the basis of variations in the optical path found in the trajectories of light rays over concentric zones whose specific mass is a function of the distance to the axis Ox.

In a section normal to Ox, ρ_0 being the value of the specific mass on the side upstream of the shock wave at a distance r_p from Ox, the value of ρ at a point T, at a distance of r_t, is given by the following formula:

$$\rho_t = \rho_0 - \frac{\lambda}{\pi a B} \int_{u_t}^{u_p} \frac{S'(u)\,du}{\sqrt{u - u_t}}, \quad \text{with } u = \bar{r}^2 \text{ and } \bar{r} = r/a. \tag{1}$$

The function $S'(u) = (1/2\bar{r})\,(dS/d\bar{r})$ is determined by measurements of the slope of curves for $N(y)$ and $\bar{N}(y)$ along each scanning line (Fig. 3).

The method of calculating (1) on the basis of the experimental curve $S'(u)$ (Fig. 4) represented by a polynomial approximation is treated in [6].

III. 3. The Nature of an Interferogram due to the Presence of a Shock in an Axisymmetric Flow.

A transparent medium whose specific mass was:

$$\rho = \rho_0 \quad \text{for } u \geq u_p$$
$$\rho = \rho_0 + \Delta\rho \quad u < u_p,$$

brought about a variation in the optical path S, represented for $u \leq u_p$ by the expression:

$$S(u) = \frac{2\,Ba}{\lambda}\,\Delta\rho\,\sqrt{u_p - u}. \qquad (2)$$

In the general case of a discontinuity in specific mass at a distance u_p from the axis of an axisymmetric flow which is non-uniform at $u < u_p$, (2) gives the expression for the limit of u_p in an increase of the optical path S.

The derivative S'(u) which has a limit of

$$\lim S'(u) = -\frac{Ba}{\lambda}\,\frac{\Delta\rho}{\sqrt{u_p - u}}, \qquad (3)$$

thus has singularity with respect to u_p. In particular, an experimental determination of S'(u) becomes illusory in the neighborhood of u_p.

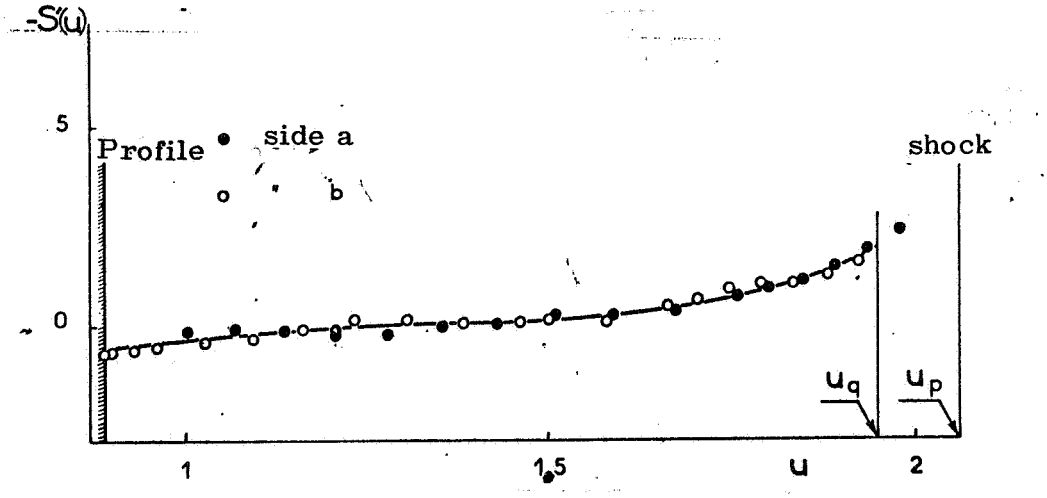

Fig. 4. Derivitive of Optical Path. Curve S'(u).

An examination of (1) shows the need for representing in suitable form the function of S'(u) beyond u_q, where a correct experimental determination of this function practically comes to a stop (Fig. 4).

This question has already been treated in the literature and has found a solution known under the name of "deshicking".

The method consists of decomposing the function S(u) in the form /35

$$S(u) = S_1(u) + S_2(u) \tag{4}$$

with:

$$S_1(u) = [\lim_{u \to u_p} (S(u)/\sqrt{u_p - u})] \sqrt{u_p - u} \tag{5}$$

i.e., according to (2):

$$S_1(u) = \frac{2\,Ba\Delta\rho}{\lambda} \sqrt{u_p - u}.$$

The relation (1) is then written as:

$$\begin{aligned} \rho_t &= \rho_0 - \frac{\lambda}{\pi Ba} \int_{u_t}^{u_p} \frac{S_1'(u)\,du}{\sqrt{u - u_t}} - \frac{\lambda}{\pi Ba} \int_{u_t}^{u_p} \frac{S_2'(u)}{\sqrt{u - u_t}}\,du \\ &= \rho_0 + \Delta\rho \qquad\qquad - \frac{\lambda}{\pi Ba} \int_{u_t}^{u_p} \frac{S_2'(u)}{\sqrt{u - u_t}}\,du. \end{aligned} \tag{6}$$

The function $S_2'(u)$ does not have singularity with u_p, and the general method of calculating (1) is applicable for it.

In order to discuss in more detail the errors which can arise in an incorrect determination of the function S over the interval (u_q, u_p), a different decomposition of (1) was used. It was then written as:

$$\rho_t = \rho_0 - \frac{\lambda}{\pi Ba} \int_{u_t}^{u_p} \frac{S'(u)\,du}{\sqrt{u - u_t}} - \frac{\lambda}{\pi Ba} \int_{u_t}^{u_p} \frac{S'(u)\,du}{\sqrt{u - u_t}}. \tag{7}$$

Under these conditions, calculations of

$$\nu = (\rho - \rho_0)\rho i_0 \tag{8}$$

resulted in the sum of two terms:

$$v = v_1 + v_2 \tag{9}$$

One, $v_1(u_t)$ was obtained according to the general method based on the function S' which was determined experimentally over the interval (u_t, u_q):

$$v_1 = -\frac{\lambda}{\pi B a \rho_{t_0}} \int_{u_t}^{u_q} \frac{S'(u)\,du}{\sqrt{u - u_t}} \tag{10}$$

The other, $v_2(u_t)$ was given by calculations of the integral

$$v_2 = -\frac{\lambda}{\pi B a \rho_{t_0}} \int_{u_q}^{u_p} \frac{S'(u)\,du}{\sqrt{u - u_t}} \tag{11}$$

Considering (3), v_2 is written thus:

$$v_2 = \int_{u_q}^{u_p} \frac{(\Delta\rho/\rho_{t_0})\,du}{\sqrt{u_p - u}\,\sqrt{u - u_t}} - \frac{\lambda}{\pi B a \rho_{t_0}} \int_{u_q}^{u_p} \frac{2(u)\,du}{\sqrt{u - u_t}} \tag{12}$$

with

$$\lim_{u = u_p} \varepsilon(u) = 0.$$

In the hypothesis with

$$S_{ref} = \frac{2Ba}{\lambda}\,\Delta\rho\,\sqrt{u_p - u}$$

as an exact representation of S between u_q and u_p, the error in v_2 which results from a replacement of S_{ref} by each of the following functions was calculated (Fig. 5):

1° $S_I = \frac{2Ba}{\lambda}\,\Delta\rho\,\sqrt{u_p^* - u}$: error in u_p;

2° $S_{II} = \frac{2Ba}{\lambda}\,\Delta\tilde{\rho}\,\sqrt{u_p - u}$: error in $\Delta\rho$;

$3^{o}\ S_{III} = \frac{2\,Ba}{\lambda}\,\Delta\rho^{*}\sqrt{u_p^{*} - u}$: errors in u_p and Δ_ρ compensated so that $S_{III}(u_q) = S_{ref}(u_q)$.

$4^{o}\ S_{IV} = \frac{2\,Ba}{\lambda}\,\Delta\tilde{\rho}\sqrt{u_p - u}$; error in Δ_ρ compensated by the term $\varepsilon(u)$ so that $S_{IV}(u_q) = S_{ref}(u_q)$.

$$+[S_{ref}(u_q) - S_{II}(uq)]\ \left(\frac{u_p - u}{u_p - u_q}\right)$$

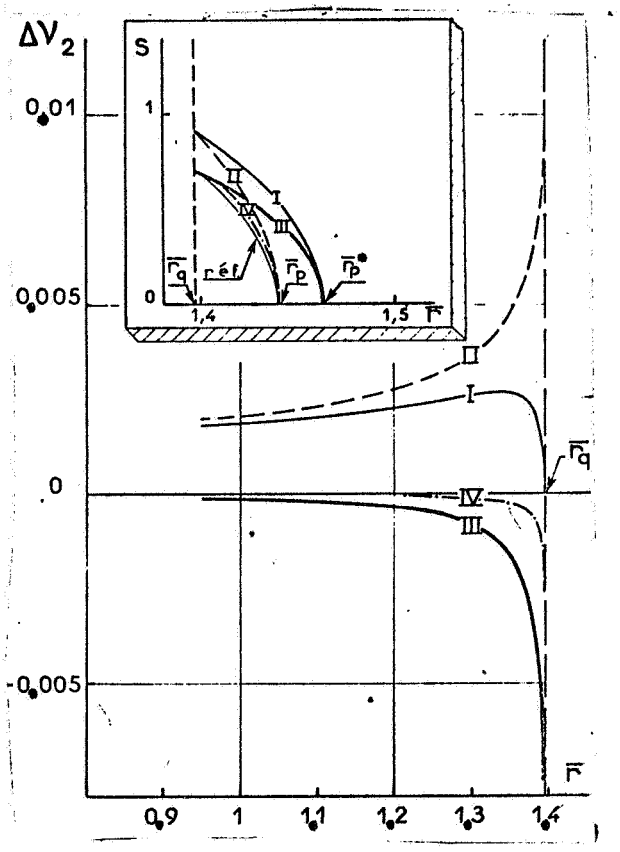

Fig. 5. Calculation of Error in ν_2.

As shown in Figure 5, errors of Type III and IV, which are compensated so that the value of S for u_q is exact, decrease rapidly, in contrast to errors I and II.

Calculations of ν_2 were thus carried out on the basis of the function S*, defined over the interval (u_q, u_p^*) and replacing the unknown exact function S over the interval (u_q, u_p); S* is determined in the following way on the basis of measurements of $S(u_q)$ and $S'(u_q)$ for u_q:

$$\begin{aligned} S^{*} &= \frac{2\,Ba}{\lambda}\,\Delta\rho^{*}\sqrt{u_p^{*} - u} \\ u_p^{*} &= u_q - \frac{S_q}{2\,S_q'} \\ \Delta\rho^{*} &= \frac{\lambda}{Ba}\sqrt{\frac{-S_q S_q'}{2}} \end{aligned} \qquad (13)$$

Under these conditions, $\nu_2(u_t)$ is expressed explicitly by the following:

$$\nu_2 = \frac{\Delta\rho^{*}}{\rho\, i_0}\ \text{Arc sin}\sqrt{\frac{u_p^{*} - u_q}{u_p^{*} - u_t}} \qquad (14)$$

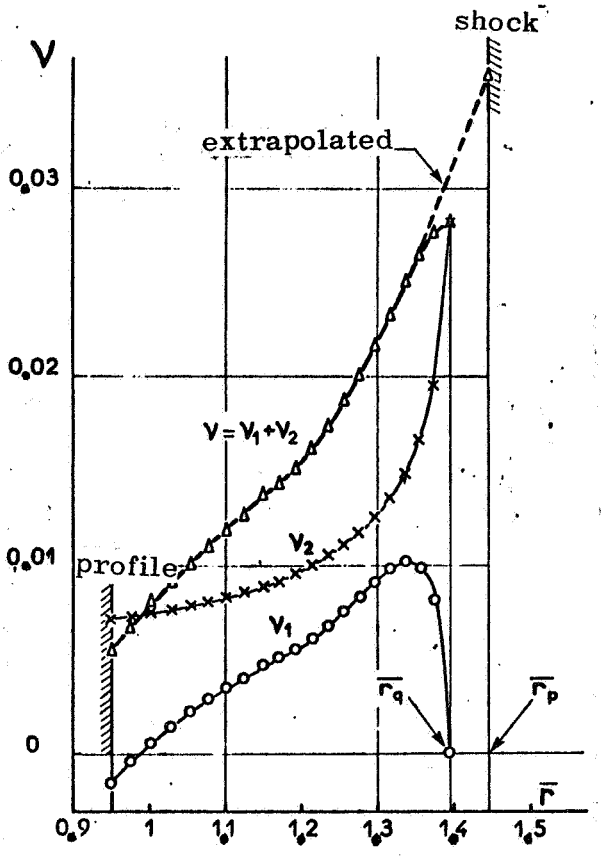

Fig. 6. Calculation of ν.

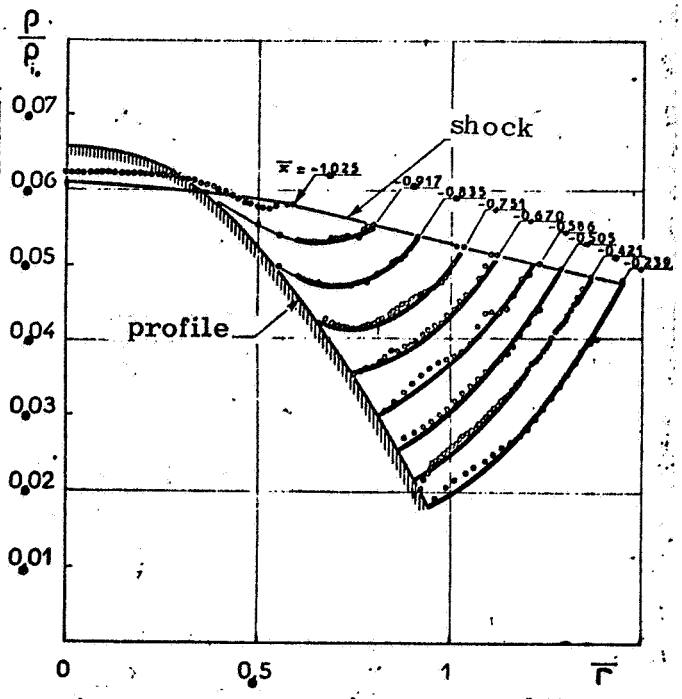

Fig. 8. Smoothing Experimental Values of $\rho/\rho_{i0} = f(\bar{r})$.

o Experimental Vauue
Smoothing Curve
Parabola

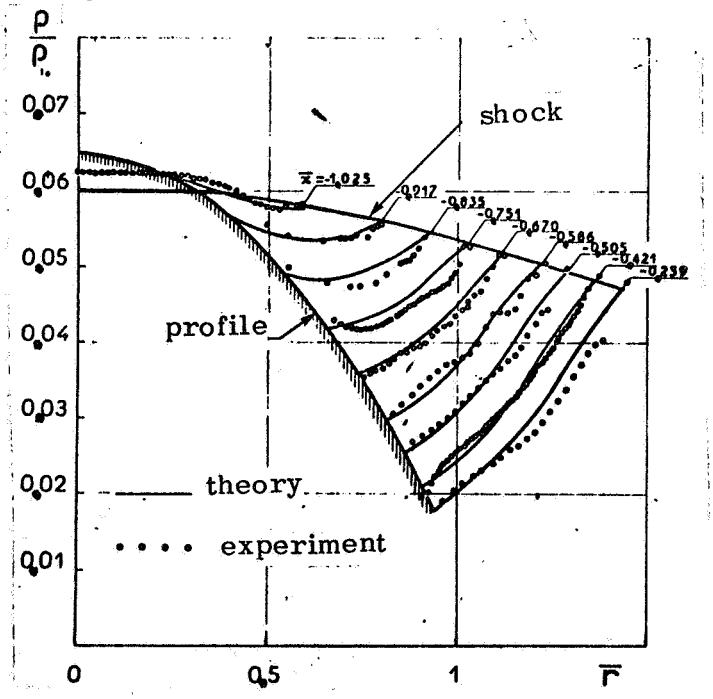

Fig. 7. Evolution of the Specific Mass. Theory
Experiment

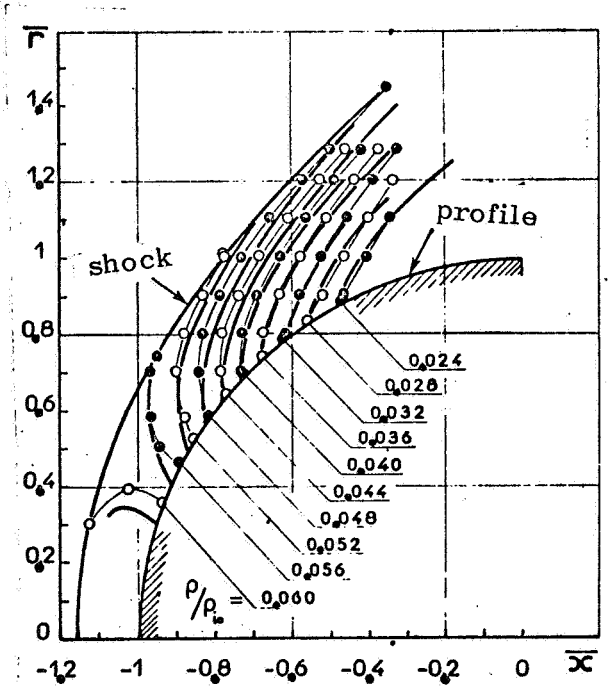

Fig. 9. Field of Specific Masses.
Theory
Experiment

The value ν is thus given by (9), (10) and (14). The values calculated for the neighborhood of u_q were not kept. In this region, ν is determined by interpolation between the calculated values for points removed from the shock (little affected by the errors considered above) and the value $\Delta\rho/\rho_i$ calculated on the basis of the Mach number and the tangent to the shock (Fig. 6). /37

III. 4. Results of Measurement.

Figure 7 shows values of $\rho/\rho_{i_0} = f(\bar{r})$ resulting from interferometric measurements along the scanning lines at $\bar{x} = Cte$.

The deviations from theory could be due in part to nonuniformity in the flow upstream of the shock, which was not considered in theoretical calculations for the average value of $M_0 = 4.94$.

The experimental values were smoothed out and approximated by a parabolic representation in the following portion of the field:

$$-1 \leq \bar{x} \leq -0.24; \quad 0.6 \leq \bar{r} \leq 1.4 \quad \text{(Fig. 8)}.$$

Figure 9 gives the physical appearance of curves for $\rho/\rho_{i_0} = Cte$, determined on the basis of the values in Figure 8 derived from the smoothing operation.

The corresponding curves for the theoretical calculation of Belotserkowsky for $M_0 = 4.94$ were given for the sake of a comparison.

IV. Calculations Of The Flow

IV. 1. Calculation Principle (Fig. 10).

The principal unknown values of the problem are the direction ϕ of the velocity, the pressure p, and entropy s for each point Q.

These values are known for every point Q_0 of the surface downstream of the shock, since the form of the latter was given experimentally.

Calculations then follow step by step on the basis of Q_0 for the characteristic value $(-\alpha)$; for this, we use:

-the characteristic relation relative to displacement $d\zeta$ over $(-\alpha)$

$$d\varphi - \frac{\sin\alpha\cos\alpha}{\gamma}\frac{dp}{p} = \frac{\sin\alpha\sin\varphi}{\bar{r}}d\zeta \qquad (11)$$

-the amount spanning $d\zeta$

$$dq = 2\pi\bar{r}\rho a\,d\zeta \qquad (12)$$

-the specific mass given by $\frac{\rho}{\rho i_0}$ $(\bar{x}, \bar{r})$.

Integration of (12) permits identification of the stream line at each point with more and more accuracy and determination of the entropy on the basis of the shock equation $\bar{r}(\bar{x})$, since the upstream flow is known.

The value of p is derived from ρ and s; integration of (11) then gives ϕ.

The progression of talculations on each characteristic stops: either on the sonic line, or on the stream line of the stop point, or on a fixed limit $\bar{x}$.

The calculations then take up the following characteristic, whose ordinate at the orgin is displaced by a fixed $\Delta\bar{r}$.

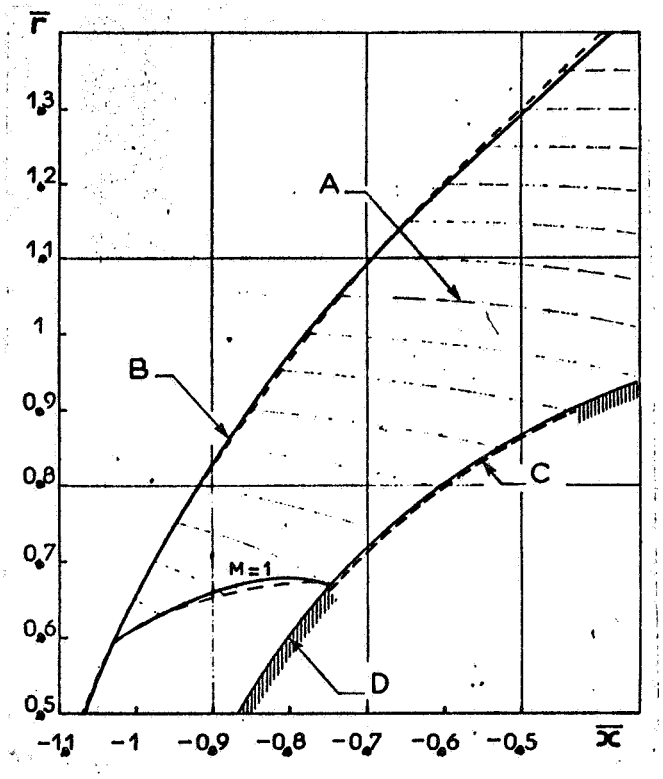

Fig. 10. Calculations of the Flow. —— ——Theory, --- Experiment. A - Characteristics -α, B - Shock, C - Stream Line at Stop Points, D - Circular Profile, $\bar{r} = 1$.

IV. 2. Results of Calculations.

The coherence of calculations thus established is confirmed by the following two results:

-the stream line constructed nearer and nearer the stop point is circular (radius equal to 0.998 ± 0.001) and very close to the real profile (circle with radius of one);

-the velocity calculated for the circle is tangential to the circle (about + 0.5°).

Figure 11 shows stream lines and iso-Mach lines of the flow distribution. The velocity vector was plotted at several points in the stream line of the stop point.

IV. 3. Simulation of Sources of Errors.

A particl modification of the calculate data aids in creating the experimental errors artifically and judging their effects (Fig. 12).

In Figure 12, the calculation of (1) corresponding to experimental data is compared to results obtained on the basis of the same distribution $\rho(\bar{x}, \bar{r})$, with changes in these data: either the Mach number for an upstream flow, assumed to be constant and equal to 4.94 in (2), or with a shock in (3).

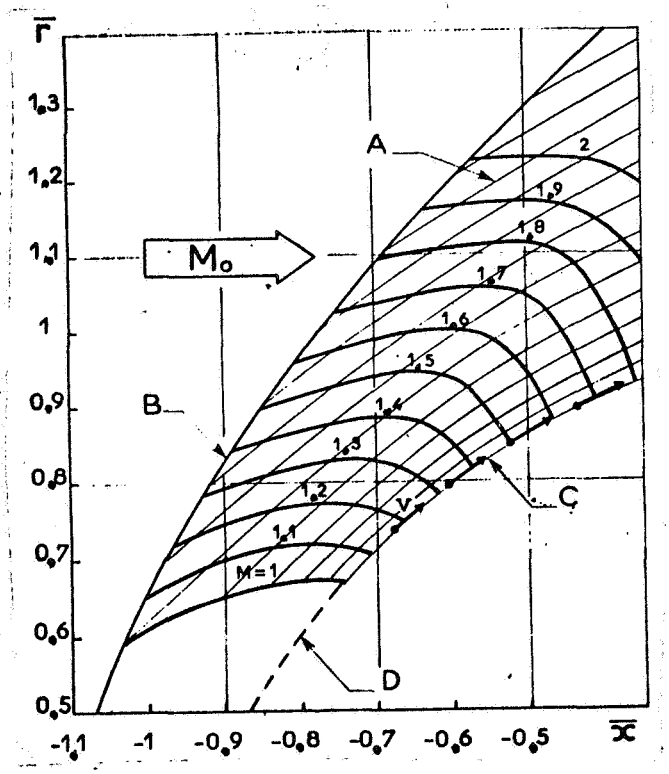

Fig. 11. Experimental Velocity Field. A - Stream Lines. B - Shock. C - Stream Line of Stop Points. D - Circular Profile, $\bar{r} = 1$.

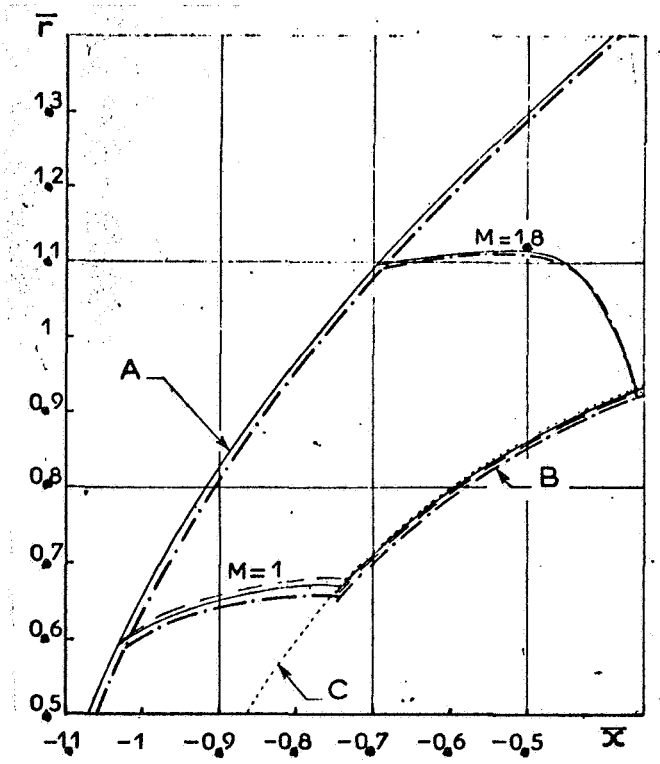

/38

Fig. 12. Discussion of Experimental Errors. ——Calculation 1. ----Calculation 2. —.—Calculation 3. A - Shock. B - Stream Line of Stop Points. C - Circle, $\bar{r} = 1$.

These sources of error have practically no effect on the shock-profile distance, and the deviations observed, which are substantial at the level of the sonic line, tend to disappear as the flow accelerates.

V. Conclusion.

This experimental study allows us to judge with a typical case the possibilities offered by the use of interferometry with a wind-tunnel in order ot obtain the local aerodynamic characteristics of a supersonic axisymmetric flow with a shock wave.

The technique of using interferograms involves a modification in the so-called "deshocking" method so as to consider the singularity due to the presence of the shockwave.

The determination of the field of specific masses carried out under these conditions, as well as the corresponding calculations of velocities, brings about a result which reproduces the theoretical values of Belotserkowsky very satisfactorily.

At the same time, the coherence of calculations established on the basis of the experimental distribution of specific mass (determination of the flow boundary) is an indirect proof of the measurement precision and accuracy in reproduction.

We should mention that this technique, which is based on a determination of the derivative $S'(u)$ of the variation in the optical path, can also be adapted, without modifications, to the case of quantitative strioscopy, which gives $S'(u)$ directly, in principle. The latter method would have precision comparable to that of interferometry provided that it could determine the deflection of light rays at about $\pm 3.10^{-5}$ rad.

A technique of applying quantitative strioscopy which was recently developed at O.N.E.R.A. by M. Philbert seems to have met these requirements. It is desirable that this be confirmed by application of this method to the above example.

SYMBOLS

x: Abscissa, reading along the axis of rotation, in the direction of the flow, origin at the center of the sphere.

r: Distance to the axis of rotation - also, ordinate in the meridian plane, normal to Ox.

a: Radius of the sphere.

$\bar{x}$, $\bar{r}$: Reduced abscissa and ordinate related to "a".

u: $\bar{r}^2$

y: Slope, of arbitrary origin, on reading line of the negative, normal to Ox.

$d\zeta$: Elementary arc over one characteristic ($-\alpha$).

v: Velocity.

ϕ: Angle between velocity and direction of the axis.

M: Marh number (M_0: Mach number upstream of the shock).

α: Mach angle. /39

s: Entropy

$p_{i_0}, T_{i_0}, \rho_{i_0}$: Pressure, temperature and specific mass for generating conditions of the upstream flow.

ρ: Specific mass (ρ_0: specific mass upstream of the shock

ν: $= \frac{\rho \ \rho 0}{\rho : 0}$

Δp: Variation in specific mass at right angles with the shock.

λ: Wavelength.

B: Gladstone constant (= 0.2262 cm^3/g for air and radiation λ 5461 Å).

N: Ordered number of fringes on the interferogram of the flow.

$\bar{N}$: Ordered number of fringes on the reference table.

S: $= (N-\bar{N})$

REFERENCES

1. Ladenburg, R., C.C. Van Voorhis and J. Winckler: Interferometric Study of Supersonic Phenomena, Part I: A Supersonic Air Jet At 60LB|IN^2 Tank Pressure. Navord Report 69/46, April 1946. Interferometric Study of Supersonic Phenomena Part II: The Gas Flow Around Various Objects In A Free Hemegeneous Supersonic Air Stream. Navord Report 93/46, September 2, 1946.
2. Gooderum, Paul B. and George P. Wood: Density Fields Around A Sphere At Mach Numbers 1.30 and 1.62. NACA - T.N. 2173, August 1950.
3. Bennett, F.D., W.C. Carter and V.E. Bergdolt: Interferometric Analysis Of Airflow About Projectiles In Free Flight. Journal Of Applied Physics Vol. 23, No. 4, April 1952.
4. Weyl, F. Joachim: Analytical Methods In Optical Examination Of Supersonic Flow. Navord Report 211-45, Bur. Ord., Navy Dept., December 11, 1945.
5. Sedney, R. and G.D. Kahl: Interferometric Study Of the Hypersonic Blunt Body Problem. Proc. Of The Fourth AFBMD/STL Symposium Advances In Ballistic Missile and Space Technology, Vol. 1 and 2, pp. 337-351, 1960.
6. Solignac, J.L.: Methode de depouillement des interferogrammes en ecoulement de revolution. (Method of Analyzing Interferograms of an Axisymmetric Flow). Rech. Aer. No. 104, 1965.
7. Belotserkowsky, O.M.: On the Calculation of Flow Past Axisymmetric Bodies with Detached Shock Waves Using an Electronic Computing Machine. PMM, Vol. 24, No. 1, pp. 511-517, 1960.
8. Kendall, Jr. James M.: Experimetns on Supersonic Blunt Body Flows. Progress Report 20-372, Jet Propulsion Laboratory Calif. Inst. Techn., February 1959.

Translated for the National Aeronautics and Space Administration by:
Aztec School of Languages, Inc.,
Research Translation Division (260)
Maynard, Massachusetts.
NASw-1692.